Electronic Supplementary Information

Rational design of Co embedded N, S-codoped carbon nanoplates as anode materials for high performance lithium-ion batteries

Wei Shuang,[a] Lingjun Kong,[a] Ming Zhong,[a] Danhong Wang,*[a] Jian Liu,[a] Xian-He Bu*[abc]

[a]School of Materials Science and Engineering, National Institute for Advanced Materials, TKL of Metal and Molecule Based Material Chemistry, Nankai University, Tianjin 300350 (P.R. China).

[b]Key Laboratory of Advanced Energy Materials Chemistry (Ministry of Education) College of Chemistry, Nankai University, Tianjin 300071 (P.R. China).

[c]Collaborative Innovation Center of Chemical Science and Engineering, Tianjin 300072, (P.R. China).

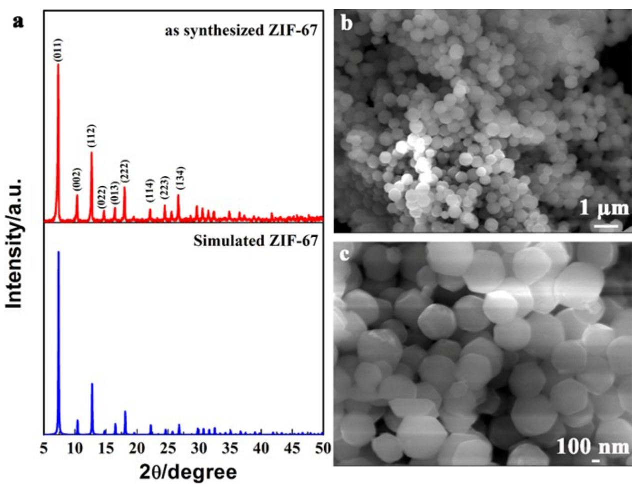

Fig. S1 (a) XRD patterns and (b, c) FE-SEM images of the ZIF-67.

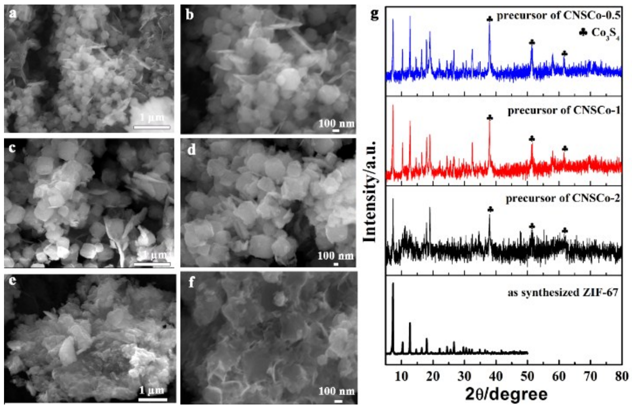

Fig. S2 FE-SEM images of the CNSCo-0.5 precursor (a, b), the CNSCo-1 precursor (c, d), the CNSCo-2 precursor (e, f) and XRD patterns of all the precursors.

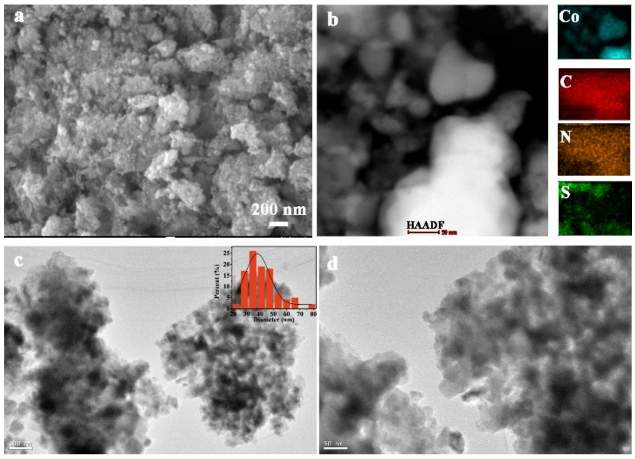

Fig. S3 (a) FE-SEM images, (b) HAADF-STEM images and (c, d) TEM images with corresponding elemental mappings of the CNSCo-2.

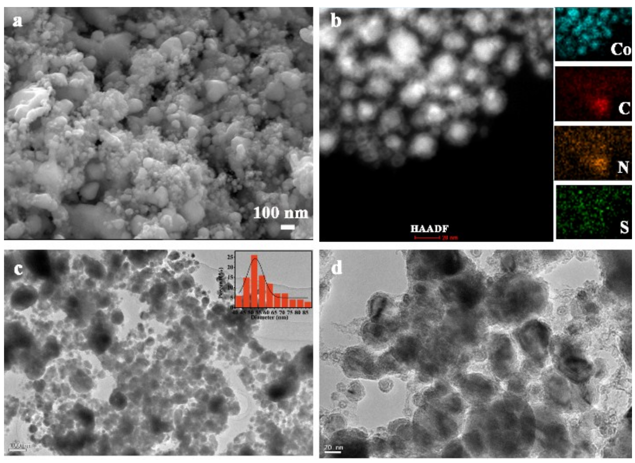

Fig. S4 (a) FE-SEM images, (b) HAADF-STEM images and (c, d) TEM images with corresponding elemental mappings of the CNSCo-1.

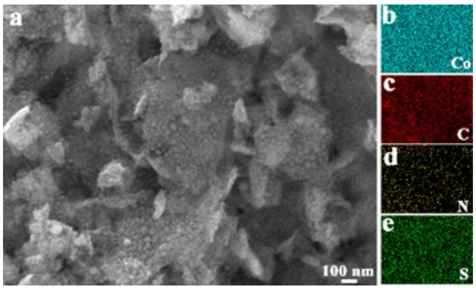

Fig. S5 (a) FE-SEM images and (b, c, d, e) corresponding elemental mappings of the CNSCo-0.5.

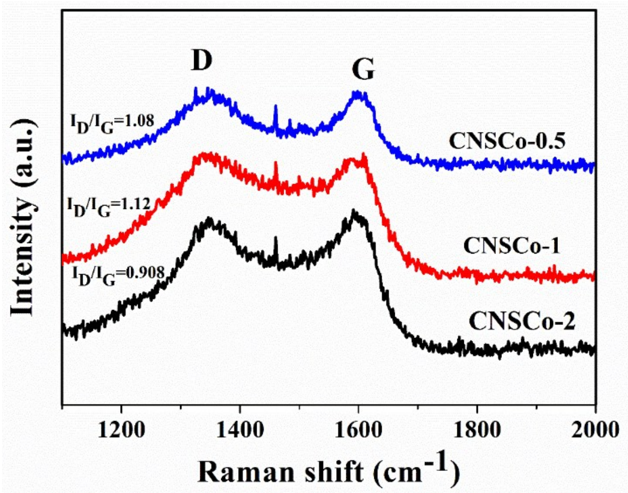

Fig. S6 Raman spectra for the CNSCo-2, CNSCo-1 and CNSCo-0.5 samples.

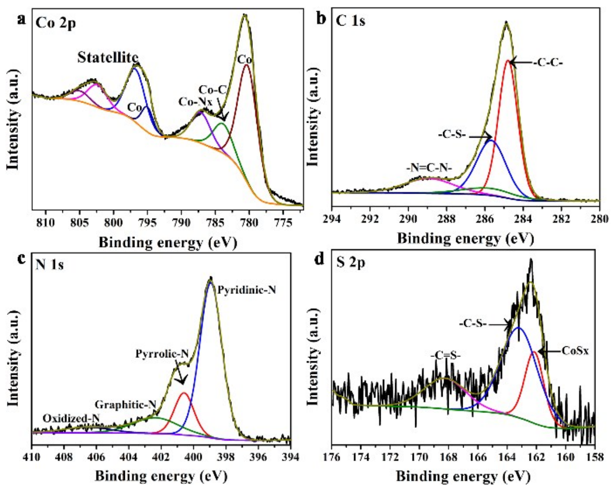

Fig. S7 High-resolution XPS spectra and fitted curves of (a) Co 2p, (b) C 1s, (c) N 1s, (d) S 2p of the CNSCo-1.

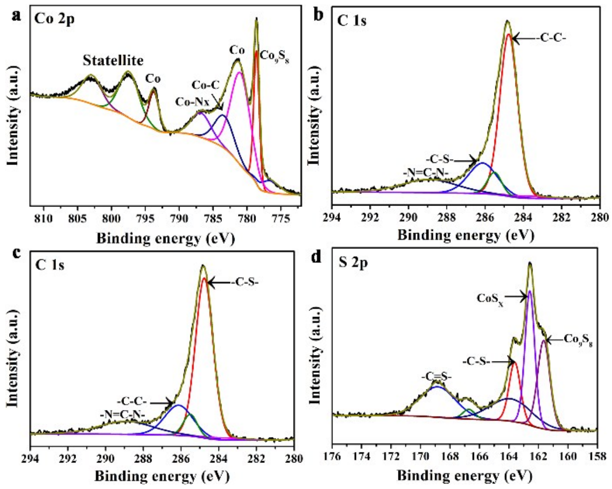

Fig. S8 High-resolution XPS spectra and fitted curves of (a) Co 2p, (b) C 1s, (c) N 1s, (d) S 2p of the CNSCo-2.

Table S1. Elemental contents of the CNSCo-2, CNSCo-1, CNSCo-0.5 from XPS.

Sample	C (at. %)	N (at. %)	S (at. %)	Co (at. %)
CNSCo-2	59.08	4.03	17.84	19.05
CNSCo-1	72.05	9.01	1.36	17.58
CNSCo-0.5	76.80	3.82	1.31	18.07

N_2 sorption measurement at 77 K was performed to analysis the specific surface area and porosity of the CNSCo-x samples (Fig. S9). The CNSCo-0.5 exhibits the highest Brunauer–Emmett–Teller (BET) specific surface area (113.13 m^2 g^{-1}) among the obtained samples, while the CNSCo-2 and CNSCo-1 have BET surface areas of 62.56 and 29.66 m^2 g^{-1}, respectively. The high BET surface area of the CNSCo-0.5 can provide a large interface to facilitate the easy uptake and release of lithium ions in electrolyte. The three obtained CNSCo-x samples all possess two-size mesoporous pores, 4.0 nm, 19.0 nm of the CNSCo-2, 2.2 nm, 13.1 nm of the CNSCo-1, 3.8 nm, 33.0 nm of the CNSCo-0.5. The mesopores of the CNSCo-2 and CNSCo-1 are from the space among non-uniform nanoparticles. The smaller mesopores originate from the space of nanoparticles while the larger mesopores may come from the space with in the carbon networks.

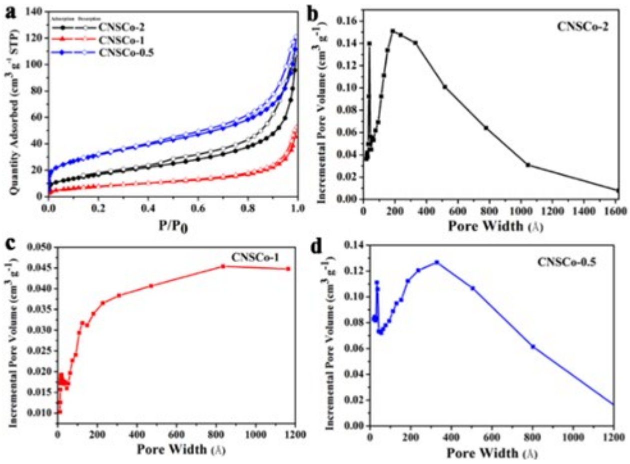

Fig. S9 (a) N_2-sorption isotherms of the CNSCo-2, CNSCo-1, CNSCo-0.5, and pore size distribution curves for (b) the CNSCo-2, (c) the CNSCo-1, and (d) the CNSCo-0.5.

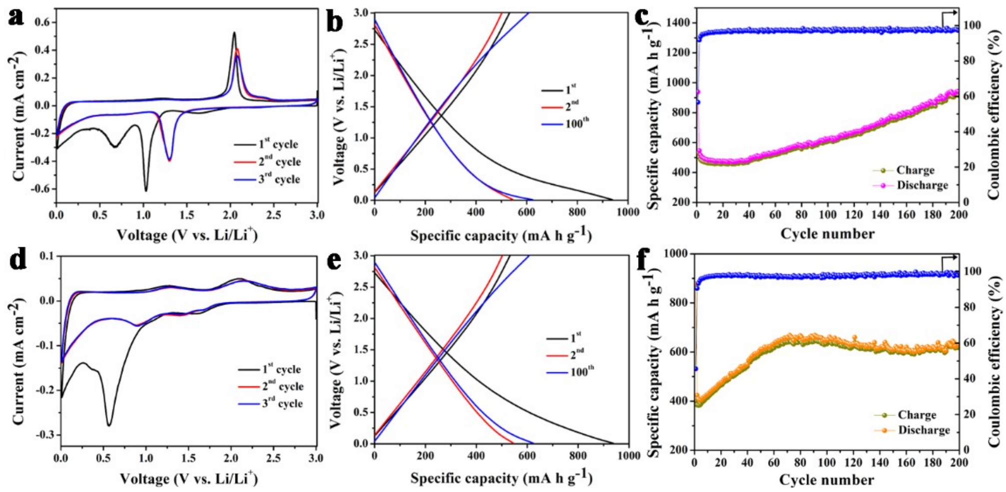

Fig. S10 (a) CV curves at a scan rate of 0.1 mV s^{-1} in the range of 0.01-3.0 V, (b) charge-discharge profiles of 1^{st}, 2^{nd}, 100^{th} cycle at current density of 200 mA g^{-1} of the CNSCo-2, (c) cycling performance and coulombic efficiency at current density of 200 mA g^{-1}, and (d) CV curves at a scan rate of 0.1 mV s^{-1} in the range of 0.01-3.0 V, (e) charge-discharge profiles of 1^{st}, 2^{nd}, 100^{th} cycle at current density of 200 mA g^{-1} of the CNSCo-1, (f) cycling performance and coulombic efficiency at current density of 200 mA g^{-1}.

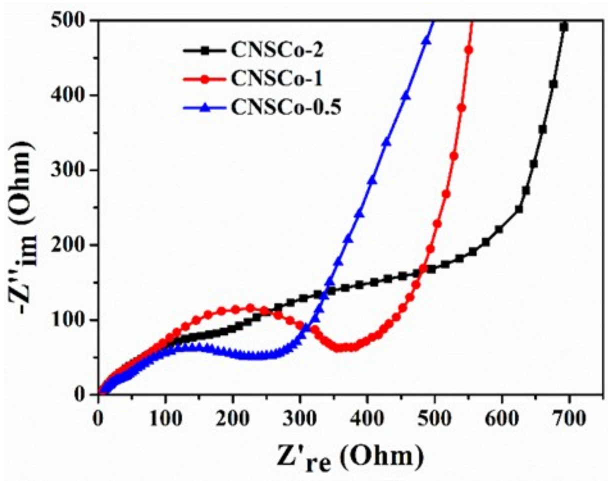

Fig. S11 EIS of the CNSCo-2, CNSCo-1, CNSCo-0.5.

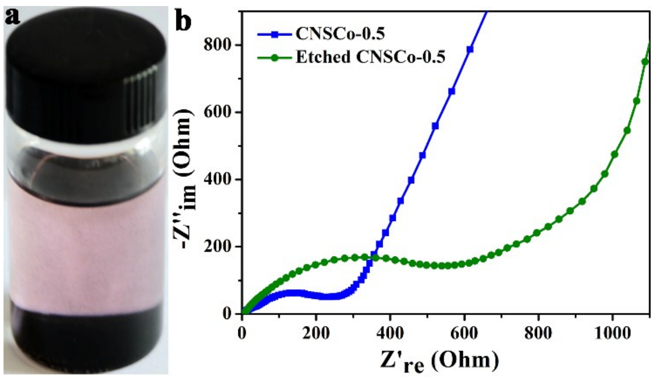

Fig. S12 (a) The photo of pink solution and (b) EIS of the CNSCo-0.5 etched by 1.0 M HCl.

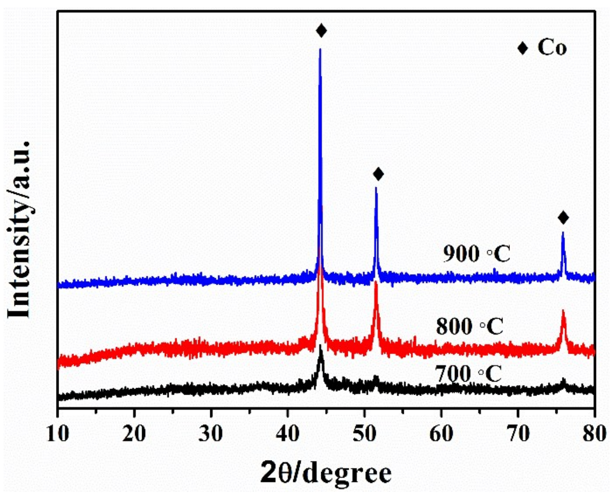

Fig. S13 XRD patterns of the CNSCo-0.5 synthesized at 700 ºC, 800 ºC and 900 ºC.

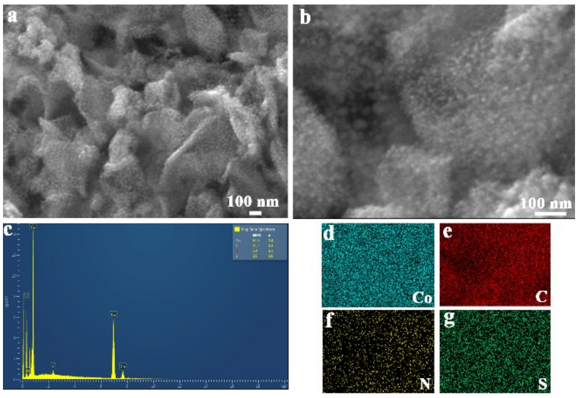

Fig. S14 (a, b) FE-SEM images, (c) EDS image and (d, e, f, g) corresponding elemental mappings of the CNSCo-0.5 synthesized at 700 ºC.

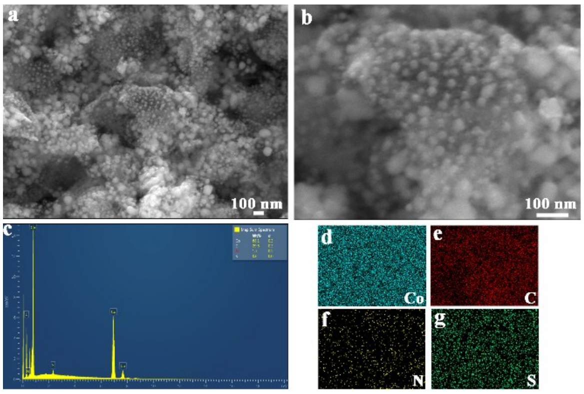

Fig. S15 (a, b) FE-SEM images, (c) EDS image and (d, e, f, g) corresponding elemental mappings of the CNSCo-0.5 synthesized at 800 ºC.

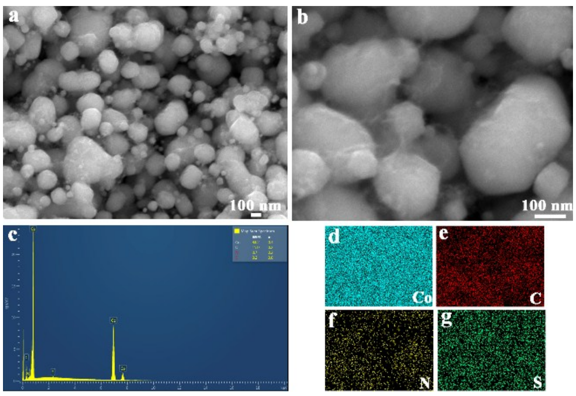

Fig. S16 (a, b) FE-SEM images, (c) EDS image and (d, e, f, g) corresponding elemental mappings of the CNSCo-0.5 synthesized at 900 ºC.

Table S2. Elemental contents of the CNSCo-0.5 synthesized at 700 ºC, 800 ºC and 900 ºC from EDS.

Sample	C (at. %)	N (at. %)	S (at. %)	Co (at. %)
700 ºC	70.32	4.10	0.38	25.20
800 ºC	65.46	3.22	0.51	30.81
900 ºC	45.68	1.83	0.22	52.27

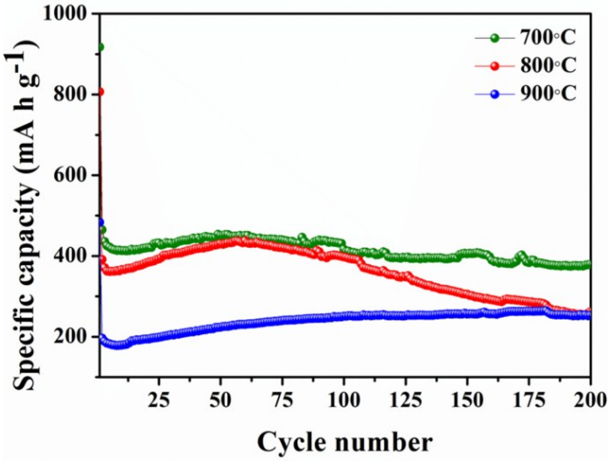

Fig. S17 Discharge capacities of the CNSCo-0.5 synthesized at 700 ºC, 800 ºC and 900 ºC.

Table S3. The electrochemical performance of heteroatom-doped carbon materials as anode materials for LIBs.

Sample	Current density (mA g^{-1})	Cycle number	Capacity (mA h g^{-1})	Ref.
CNSCo-0.5	200	200	1360.4	Our work
N-C octahedral particles	100	100	890	1
NS-C films	200	2000	357.2	2
NSDPC	100	50	864	3
NFCs	100	300	645	4
NPCMs	100	400	655.1	5
C60@N-MPC	1000	400	1077	6
3D NS-GSs	100	80	1117	7
N-doped graphene	50	30	827	8

References

1 Y. Yang, F. Zheng, G. Xia, Z. Lun, Q. Chen, *J. Mater. Chem. A*, 2015, **3**, 18657.

2 J. Ruan, T. Yuan, Y. Pang, S. Luo, C. Peng, J. Yang, S. Zheng, *Carbon*, 2018, **126**, 9.

3 Z. Qiu, Y. Lin, H. Xin, P. Han, D. Li, B. Yang, P. Li, S. Ullah, H. Fan, C. Zhu, J. Xu, *Carbon*, 2018, **126**, 85.

4 Q. Wu, J. Liu, C. Yuan, Q. Li, H. G. Wang, *Appl. Surf. Sci.*, 2017, **425**, 1082.

5 H. G. Wang, C. Yuan, R. Zhou, Q. Duan, Y. Li, *Chem. Eng. J.*, 2017, **316**, 1004.

6 J. Guan, X. Zhong, X. Chen, X. Zhu, P. Li, J. Wu, Y. Lu, Y. Yu, S. Yang, *Nanoscale*, 2018, **10**, 2473.

7 D. Sun, J. Yang, X. Yan, *Chem. Commun.*, 2015, **51**, 2134.

8 Z. S. Wu, W. C. Ren, L. Xu, F. Li, H. M. Cheng, *ACS Nano*, 2011, **5**, 5463.